Exact Analysis of DDS Spurs and SNR due to Phase Truncation and Arbitrary Phase-to-Amplitude Errors

Arthur Torosyan
Electrical Engineering Department
University of California, Los Angeles (UCLA)
Los Angeles, USA
torosyan@alum.mit.edu

Alan N. Willson, Jr.
Electrical Engineering Department
University of California, Los Angeles (UCLA)
Los Angeles, USA
willson@ee.ucla.edu

Abstract—**This paper presents the theoretical basis for an algorithm that performs an *exact* analysis of the output spectrum of Direct Digital Frequency Synthesizers (DDS or DDFS) in the presence of phase accumulator truncation, finite arithmetic precision and arbitrary approximations and errors in the sine/cosine mapping function (SCMF). The derivation provides strong insight into spurious frequency (spur) magnitude and spectral location, and makes evident that the set of spurs due to phase-word truncation and the set resulting from SCMF imprecision and errors are effectively disjoint. Phase-truncation spurs are shown to have distinct magnitudes and their spectral locations, ordered from largest to smallest in magnitude, are easily ascertained. Without generating all spur magnitudes, the algorithm supported by this theory is capable of exactly computing the Signal-to-Noise Ratio (SNR) and Spurious-Free Dynamic Range (SFDR) and exactly computing the magnitudes and locations of the N worst (i.e., largest-magnitude) spurs or all spurs with magnitudes larger than ε, due to the combined effect of phase truncation *and* arbitrary SCMF imprecision (where N and ε are user-specified parameters).**

I. Introduction[1]

The general structure of a DDS, depicted in Fig. 1, was first introduced in 1971 by Tierney, Rader, and Gold [3]. The DDS can be partitioned into two functional units. The first, the phase accumulator, consisting of an overflowing adder and a feedback register, accumulates the input frequency control word (fcw) to produce a phase angle for the sine/cosine mapping function (SCMF), which is the second functional unit. The SCMF can be viewed as a mapper (e.g., lookup table) between an input phase angle θ and its corresponding $\sin\theta$ and $\cos\theta$ values. Various efficient implementations have been proposed for this mapping function, e.g., [4], [5], but we need only consider that, however implemented, it is simply a mapping from the input angle θ to $\sin\theta$ and/or $\cos\theta$.

To reduce the SCMF implementation complexity, the phase accumulator output typically is truncated before being fed to the SCMF, as shown in Fig. 1, where only W bits out of M bits are retained. This phase truncation causes errors (deterministic, periodic errors, often referred to as noise) at

This research was supported by Analog Devices, Broadcom, Globespan, and Rockwell Scientific through UC MICRO Grants 00-104 and 01-100 and by an Intel Corporation Ph.D. Fellowship.

[1]This article extends the fundamental theory and corrects equation (1) in Section 3 of the paper presented at the *2-nd Image and Signal Processing and Analysis Conference* in 2001, [1]. A more thorough and complete treatment of this subject can be found in [2].

0-7803-9052-0/05/$20.00 © 2005 IEEE.

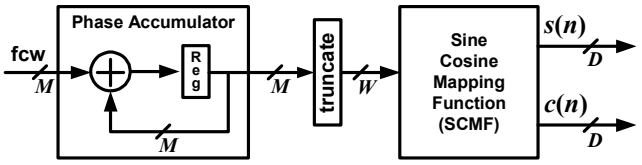

Figure 1. The general structure for DDS.

the DDS output which manifest themselves as a set of spurious frequencies (output signal components at undesired frequencies,) often referred to as spurs. Furthermore, practical implementations of the SCMF have finite precision outputs and their implementation may employ algorithmic approximations and quantization and other non-ideal operations that collectively give rise to errors specific to the SCMF implementation, e.g. [4], [5]. These SCMF errors are collectively referred to as SCMF non-idealities, and they also generate deterministic noise at the DDS output and hence contribute another set of spurs.

Early efforts for determining the magnitude and spectral location of (only) *phase-truncation spurs* were reported in 1983 by Mehrgardt [6] and later in 1985 by Nicholas [7], and in 1987 by Nicholas and Samueli [8]. These publications describe similar approaches and base their analyses on the phase-error sequence due to phase truncation and, using properties of this error sequence along with the assistance of small-angle approximations, derive a complex procedure for the characterization of phase-truncation spurs. Shortly thereafter, Jenq [9] used an elegant approach, one for analyzing a class of non-uniformly sampled signals, to model the phase error due to phase truncation and, without approximations, derived an expression for magnitudes of (only) phase-truncation spurs. In 1993 Kroupa [10] used an approach similar to that of [6], [7], and [8] and presented an algorithm for the *estimation* of phase-truncation spurs with the introduction of more approximations. None of [6], [7], [8], [9], and [10] considers the exact characterization of spurs due to *arbitrary* SCMF non-idealities, since the theories developed are derived solely from the properties of phase-truncation error. Two DDS with exactly the same top-level design parameters (i.e., M, W, and D values,) but different implementations for the SCMF can have very different SCMF non-idealities, hence, yield very different sets of spurs.

As we will show subsequently, the *overwhelming* majority of spurs generated by a DDS are those caused by SCMF non-idealities. With the exception of [1] and [2], since no algorithm to date has been reported for the exact

characterization of spurs due *both* to phase-truncation and *arbitrary* SCMF non-idealities, naturally, there is as yet no algorithm for the characterization of the N worst spurs and/or exact computation of SFDR and SNR for an *arbitrary* DDS—expect for the "brute force" approach of generating *all* spurs via simulations and searching for the worst ones. Without such an algorithm, the computational and storage requirements to generate all of the spurs are, to say the least, daunting, and likely infeasible [2].

In this paper we extend the fundamental theory of [1] and obtain a "super-efficient" algorithm, that can be applied to *any* DDS having the general structure of Fig. 1 (i.e., *any* SCMF implementation,) that:

- accepts all relevant SCMF implementation details via the "signature sequence," i.e., the sequence of 2^W samples generated by the SCMF for the 2^W possible SCMF inputs,
- without computing all spur magnitudes, and
- for all phase-truncation-causing fcw and due to the combined effect of phase truncation and the errors of the specified SCMF,
- exactly computes the SFDR and SNR, and
- exactly computes the magnitudes and locations of N largest-magnitude spurs (where N is a user-specified integer,) or all spurs with magnitudes greater than ε (where ε is a user-specified threshold.)

More detailed and thorough treatment of the development and application of this theory can be found in [2]. The analysis for the relatively simpler case of fcw that do not generate phase truncation and the consideration of all relevant initial phases in this case, are also reported in [2].

II. Basis Sets for All Spurs

For an arbitrary fcw1 and the fcw2 comprised of all zeros except for the bit at the position corresponding to the rightmost non-zero bit of fcw1, it is shown in [1] and [2] that the DDS output sequences corresponding to fcw1 and fcw2 have *identical period* and they are *simple rearrangements of each other*. For example, if fcw1 = 0101101000, then fcw2 = 0000001000, where the rightmost non-zero bit position is denoted by L and underlined at $L = 7$ for the above fcw1 and fcw2 (position is counted from MSB to LSB beginning at position 1 for the MSB). The DDS output has a period of 2^L samples, hence for the above example the DDS output has a period of $2^7 = 128$ samples. Let $s_1(n)$ and $s_2(n)$ denote the DDS output sequences due to any fcw1 and it's corresponding single-nonzero-bit fcw2, respectively, where n is the sample index. Using the normalized $\overline{\text{fcw1}}$ obtained from fcw1 by omitting all of the LSB zero bits following position L and the smallest positive integer J satisfying $\left(\overline{\text{fcw1}} \times J\right)_{\text{mod } 2^L} = 1$, the rearrangements generating s_1 from s_2 and s_2 from s_1 are shown in [1] and [2] to be

$$s_1(n) = s_2\left(\left(n \times \overline{\text{fcw1}}\right)_{\text{mod } 2^L}\right); \quad s_2(n) = s_1\left(\left(n \times J\right)_{\text{mod } 2^L}\right) \qquad (1)$$

where $(\bullet)_{\text{mod } 2^L}$ denotes a modulo operation. The interpretation of (1) is that the s_1 sequence is obtained by picking terms from the s_2 sequence in steps of $\overline{\text{fcw1}}$ and wrapping around to the beginning of the s_2 sequence when reaching its end. Similarly, the s_2 sequence is obtained by picking terms from the s_1 sequence in steps of J and wrapping around to the beginning of the s_1 sequence when reaching its end. For the example fcw1 = 0101101000 and the corresponding fcw2 = 0000001000 the normalized $\overline{\text{fcw1}} = 0101101$ (decimal value 45) and $J = 37$. Applying (1) the rearrangement of s_2 that yields s_1 is $s_1(n) = s_2\left((n \times 45)_{128}\right)$ and the rearrangement of s_1 that yields s_2 is $s_2(n) = s_1\left((n \times 37)_{128}\right)$.

Since we are interested in the spectra of the DDS outputs, we need to investigate the relationship between the Discrete Fourier Transforms (DFT) of $s_1(n)$ and $s_2(n)$. It was shown in Section 2.3 of [2] that the shortest proper length for the DFT is 2^L points (i.e., one full period of the DDS output sequence). Let S_1 and S_2 denote the 2^L-point DFT vectors of s_1 and s_2, respectively. Then, $S_1 = \mathbf{W}s_1$ and $S_2 = \mathbf{W}s_2$, where $\mathbf{W} \equiv \mathbf{W}_{2^L}$ is the $2^L \times 2^L$ matrix with $\mathbf{W}(k,n) = e^{-j\frac{2\pi}{2^L}kn}$ for $k, n = 0,\ldots,2^L - 1$.

To establish the relationship between the spectra S_1 and S_2 we first observe that the matrix $\mathbf{H}$ obtained from $\mathbf{W}$ by replacing the n-th *column* of $\mathbf{W}$ with *column* $(n \times \overline{\text{fcw1}})_{\text{mod } 2^L}$, for $n = 0,\ldots,2^L - 1$, can also be obtained from $\mathbf{W}$ by replacing the k-th *row* of $\mathbf{W}$ with *row* $(k \times \overline{\text{fcw1}})_{\text{mod } 2^L}$, for $k = 0,\ldots,2^L - 1$. Proof: The value of the element in position (k, n) of $\mathbf{H}$ obtained from *column* rearrangement of $\mathbf{W}$ is $e^{-j\frac{2\pi}{2^L}k\left(n \times \overline{\text{fcw1}}\right)_{\text{mod } 2^L}}$. Since the integer part of $\frac{1}{2^L}k\left(n \times \overline{\text{fcw1}}\right)_{\text{mod } 2^L}$ contributes nothing to this expression, it can be rewritten as $e^{-j\frac{2\pi}{2^L}\left(k\left(n \times \overline{\text{fcw1}}\right)_{\text{mod } 2^L}\right)_{\text{mod } 2^L}} = e^{-j\frac{2\pi}{2^L}n\left(k \times \overline{\text{fcw1}}\right)_{\text{mod } 2^L}}$, which is the value of the element in position (k, n) obtained from *row* rearrangement of $\mathbf{W}$. The last step relies on the identity $(a_{\text{mod } c}\, b_{\text{mod } c})_{\text{mod } c} = (ab)_{\text{mod } c}$. □ Hence, performing the inverse rearrangement on *either* the rows or columns of $\mathbf{H}$, i.e. replacing the n-th column of $\mathbf{H}$ with column $\left(n \times J\right)_{\text{mod } 2^L}$ for $n = 0,\ldots,2^L - 1$, or replacing the k-th row of $\mathbf{H}$ with row $\left(k \times J\right)_{\text{mod } 2^L}$ for $k = 0,\ldots,2^L - 1$, will reproduce the DFT matrix $\mathbf{W}$.

Now let us consider the matrix equation $v = \mathbf{M}u$, where v and u are column vectors while $\mathbf{M}$ is a square matrix. Rearranging the elements of vector u and performing the same rearrangement on the *columns* of $\mathbf{M}$ will leave the

resulting vector v unchanged. Finally, leaving u unchanged and rearranging the *rows* of **M** will similarly rearrange the elements of v.

Consider the spectrum $S_2 = \mathbf{W}s_2$ and perform the forward rearrangement (by $\overline{\text{fcw1}}$) on the elements of s_2 and the columns of **W** to produce the following expression: $S_2 = \mathbf{H}s_1$. Next, perform the inverse rearrangement (by J) on the rows of **H** to change **H** back to **W** and reproduce $S_1 = \mathbf{W}s_1$. Since the row rearrangement on **H** rearranges the elements of S_2 we conclude that S_1 is obtained by performing an inverse rearrangement on the elements of S_2. Consequently, S_2 is obtained by performing a forward rearrangement on the elements of S_1. This result is also reported in [11]. Summarizing:

$$\boxed{\begin{aligned} &s_1(n) = s_2\left(\left(n\times\overline{\text{fcw1}}\right)_{\bmod 2^L}\right);\quad s_2(n) = s_1\left((n\times J)_{\bmod 2^L}\right) \\ &S_1(k) = S_2\left((k\times J)_{\bmod 2^L}\right);\qquad S_2(k) = S_1\left(\left(k\times\overline{\text{fcw1}}\right)_{\bmod 2^L}\right) \end{aligned}} \tag{2}$$

The set of spur magnitudes created by fcw1 is *identical* to the set created by fcw2; the spurs are simply rearranged in frequency. Therefore, the set of spurs created by *any* frequency control word is a rearrangement of *one* of the M sets of spectra corresponding to the M distinct frequency control words having a single nonzero bit. These M sets of spectra can be viewed as basis sets.

III. Phase-Word Truncation

As shown in Fig. 1, the phase sequence at the output of the phase accumulator is truncated to W bits before addressing the SCMF. Consequently, all input frequency control words can be grouped into two categories. (Recall that we denote the MSB bit position as position 1.) The first group includes all fcw with their rightmost nonzero bit position L *at or before* position W, i.e. $L \le W$. In this case there will be no phase truncation and *all* spurs at the DDS output will be due to only the non-ideal SCMF. DDS behavior for such fcw can be found in [2]. The second group includes all fcw with $L > W$, and for such fcw there will be phase truncation. This paper presents the analysis of DDS spurs for fcw with $L > W$.

Let us consider, for example, a DDS with a 24-bit fcw, and a 15-bit SCMF input. In Fig. 1, this corresponds to M = 24 and W = 15. To analyze the DDS output spectrum for any fcw with L = 20, for example, as discussed in Section II, we can consider the single-nonzero-bit frequency control word fcw = 00000000000000*00001*0000, where the single nonzero bit is at position L = 20 and the 15 MSB bit positions retained at the input of the SCMF are underlined. The rightmost nonzero bit is therefore $B = L - W = 5$ bits after the truncation position W = 15. The four LSB bits could be omitted since they do not impact the outcome, and after such normalization we notice that the sequence q at the output of the phase accumulator will increment by one on every cycle. The corresponding sequence q' at the output

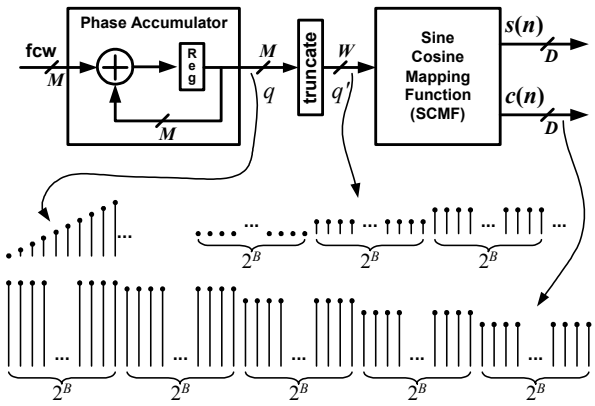

Figure 2. DDS sequences due to phase truncation.

of the truncate block will step once for every $2^B = 2^5 = 32$ cycles. In other words, it will be 0 for 32 cycles, then it will be 1 for 32 cycles, then 2 for 32 cycles, and so forth. Since the SCMF simply maps the input angle to its corresponding outputs, the same "redundant" behavior can be observed at the DDS outputs $s(n)$ and $c(n)$. Notice that the SCMF will go through all possible 2^W inputs and their corresponding outputs, each repeated 2^B times, before repeating the cycle again. Fig. 2 illustrates these properties.

To continue the discussion of phase-word truncation, let us consider again the case with $M = 24$, $W = 15$, $B = 5$ and assume that the SCMF is ideal (with infinite precision outputs). Once we gain a firm understanding of the spurs generated from phase-word truncation, the analysis will be extended to include arbitrary SCMF non-idealities. As illustrated in Section II, to obtain the basis set of spur magnitudes for all fcw with L = 20, we need to perform a 2^{20}-point DFT on the DDS output corresponding to the single-nonzero-bit fcw = 00000000000000*00001*0000. Using $s(n)$ and $S(k)$ to denote the DDS output and its corresponding spectrum obtained via 2^{20}-point DFT, respectively, we obtain

$$S(k) = \sum_{n=0}^{2^{20}-1} s(n)e^{-j\frac{2\pi}{2^{20}}nk} \quad \text{where } 0 \le n,k < 2^{20}. \tag{3}$$

Expanding (3) as 32 (in general, 2^B) summations we get:

$$S(k) = \sum_{n=0}^{2^{15}-1} s(32n)e^{-j\frac{2\pi}{2^{20}}(32n)k} + \sum_{n=0}^{2^{15}-1} s(32n+1)e^{-j\frac{2\pi}{2^{20}}(32n+1)k}$$
$$+ \ldots$$
$$+ \sum_{n=0}^{2^{15}-1} s(32n+30)e^{-j\frac{2\pi}{2^{20}}(32n+30)k} + \sum_{n=0}^{2^{15}-1} s(32n+31)e^{-j\frac{2\pi}{2^{20}}(32n+31)k}$$

where $0 \le k < 2^{20}$, $0 \le n < 2^{15}$ which, by factoring expressions not depending on n out of the summations, and writing $32/2^{20} = 1/2^{15}$, becomes:

$$S(k)=\sum_{n=0}^{2^{15}-1}s(32n)e^{-j\frac{2\pi}{2^{15}}nk}+e^{-j\frac{2\pi}{2^{20}}k}\sum_{n=0}^{2^{15}-1}s(32n+1)e^{-j\frac{2\pi}{2^{15}}nk}$$
$$+\ \ldots\ +e^{-j\frac{2\pi}{2^{20}}31k}\sum_{n=0}^{2^{15}-1}s(32n+31)e^{-j\frac{2\pi}{2^{15}}nk} \qquad (4)$$
$$\text{for } 0\le k<2^{20}.$$

Using $s(32n) = s(32n + 1) = \ldots = s(32n + 31)$, as discussed previously (Fig. 2), we can again rewrite (4) as:

$$S(k)=\left(1+e^{-j\frac{2\pi}{2^{20}}k}+\ldots+e^{-j\frac{2\pi}{2^{20}}31k}\right)\sum_{n=0}^{2^{15}-1}s(32n)e^{-j\frac{2\pi}{2^{15}}nk}$$
$$=(1+e^{-j\frac{2\pi}{2^{20}}k}+e^{-j\frac{2\pi}{2^{20}}2k}+\ \ldots\ +e^{-j\frac{2\pi}{2^{20}}31k})S'(k)$$
$$\text{for}\ \ 0\le k<2^{20}$$

where $S'(k)$ is the 2^{15}-point DFT of the non-redundant subsequence $s'(n)=s(32n)$. Thus, by summing the finite geometric series, we obtain:

$$S(k)=V(k)S'(k) \qquad (5)$$

where $V(k)=\frac{1-e^{-j\frac{2\pi}{2^{15}}k}}{1-e^{-j\frac{2\pi}{2^{20}}k}}$. Notice that, if the SCMF is implemented as a lookup table, $s'(n)$ corresponds to the contents of the table at address n. For our particular example, the SCMF would have 2^{15} entries since we chose $W = 15$. We shall refer to $V(k)$ as the windowing function. Clearly, the entire derivation for $S(k)$ and $V(k)$ in (5) can be carried out with the variables W and B instead of 15 and 5 as in our example, in which case one obtains the following general expressions for $S(k)$ and $V(k)$:

$$\begin{aligned}
&S'_W(k)=\sum_{n=0}^{2^W-1}s'(n)e^{-j\frac{2\pi}{2^W}nk} && k=0,1,\ldots,2^{W+B}-1\\
&V_{W,B}(k)=\frac{1-e^{-j\frac{2\pi}{2^W}k}}{1-e^{-j\frac{2\pi}{2^{(W+B)}}k}} && k=0,1,\ldots,2^{W+B}-1\\
&S_{W,B}(k)=V_{W,B}(k)S'_W(k) && k=0,1,\ldots,2^{W+B}-1
\end{aligned} \qquad (6)$$

where $S'_W(k)$ is periodic in k with period 2^W and one period of $V_{W,B}(k)$ windows over 2^B periods of $S'_W(k)$.

IV. Spurs due to Phase-Word Truncation

At this point we have all the necessary tools to address the assessment of spurs at the output of the DDS. To begin the discussion on the meaning of the windowing function $V_{W,B}(k)$ let us make a few comments regarding $S'_W(k)$ (which is windowed by V). When employing the assumption of an ideal SCMF (with infinite precision outputs) the expressions for $S'_W(k)$ and $|S'_W(k)|$ are quite simple. Generally, DDS can generate cosine only, sine only, or cosine and sine outputs and we refer to them as cosine DDS, sine DDS, or quadrature DDS, respectively. Without loss in generality, assuming an ideal sine DDS, $s'(n)$ is the sine output of the SCMF with frequency $\frac{2\pi}{2^W}$ radians per sample. Therefore, for $s'(n)=\sin\frac{2\pi n}{2^W}$ we have:

$$S'_W(k)=\sum_{n=0}^{2^W-1}\left(\sin\tfrac{2\pi n}{2^W}\right)e^{-j\frac{2\pi}{2^W}nk}=\sum_{n=0}^{2^W-1}\left(\frac{e^{j\frac{2\pi}{2^W}n}-e^{-j\frac{2\pi}{2^W}n}}{2j}\right)e^{-j\frac{2\pi}{2^W}nk}$$
$$=\frac{1}{2j}\sum_{n=0}^{2^W-1}\left(e^{-j\frac{2\pi}{2^W}(k-1)n}-e^{-j\frac{2\pi}{2^W}(k+1)n}\right)$$

and, using the well-known relationship

$$\sum_{n=0}^{M-1}e^{-j\frac{2\pi}{M}nl}=\begin{cases}M & \text{if } l \text{ is an integer multiple of } M\\ 0 & \text{if } l \text{ is any other integer}\end{cases}$$

we have $S'_W(k)=\frac{1}{2j}\left(2^W\delta(k-1)-2^W\delta(k-(2^W-1))\right)$. Hence, for either an ideal sine or ideal cosine DDS:

$$|S'_W(k)|=2^{W-1}\delta(k-1)+2^{W-1}\delta(k-(2^W-1)) \qquad (7)$$

where $\delta(0)=1$ and $\delta(k)=0$ for $k\neq 0$.

We now recall (see (3)) that $S_{W,B}(k)$ is periodic in k with period 2^{W+B} and it is the result of multiplying $S'_W(k)$ with $V_{W,B}(k)$ (see (6)). It is easy to verify that $V_{W,B}(k)$ is periodic in k with period 2^{W+B}. From (6):

$$V_{W,B}(k+2^{W+B})=\frac{1-e^{-j\frac{2\pi}{2^W}(k+2^{W+B})}}{1-e^{-j\frac{2\pi}{2^{(W+B)}}(k+2^{W+B})}}$$
$$=\frac{1-e^{-j\frac{2\pi}{2^W}k}e^{-j\frac{2\pi}{2^W}2^W2^B}}{1-e^{-j\frac{2\pi}{2^{(W+B)}}k}e^{-j\frac{2\pi}{2^{(W+B)}}2^{W+B}}}=V_{W,B}(k).$$

Therefore, one period of V includes (i.e., windows over) 2^B periods of $S'_W(k)$. Notice that in the case when $B = 0$, which means there is no phase-word truncation, $V_{W,B}(k)=1$ and, of course, with no phase-word truncation there is no phase-truncation distortion, hence $S_{W,B}(k)=S'_W(k)$. When $B > 0$ however, $V_{W,B}(k)$ will assume some nontrivial shape and, by windowing $S'_W(k)$, it will introduce spurious frequencies at the locations of the deltas in $S'_W(k)$ for all $|k| \neq 1$. The deltas at $k=\pm1$ will also be attenuated by the magnitude of $V_{W,B}(1)$. To demonstrate these points, consider the case for $B = 2$. That is, assume we have a frequency

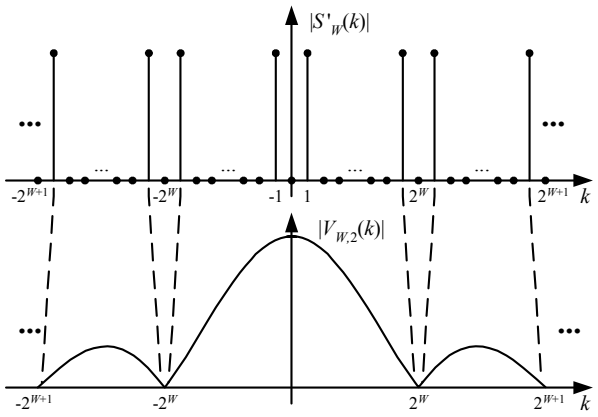

Figure 3. Windowing function $V_{W,2}(k)$ over $S'_W(k)$.

control word with its rightmost nonzero bit at position $W + 2$. Recall that $S'_W(k)$ and $S_{W,2}(k)$ are periodic in k with periods 2^W and 2^{W+2} respectively. Therefore, $S_{W,2}(k)$ can be constructed by considering four periods of $S'_W(k)$ and windowing them with $V_{W,2}(k)$, as depicted in Fig. 3. Since we know the locations of the deltas in $S'_W(k)$ not only do we know the *locations* of the spurs created from phase truncation, we also know the *exact* spur *magnitudes* since we can evaluate the windowing function V for the values of k corresponding to the locations of the deltas in $S'_W(k)$. More precisely, the magnitude of the spurious frequency at k, corresponding to the locations of the deltas, relative to that of the desired sinusoid, is $\frac{|S_{W,B}(k)|}{|S_{W,B}(1)|} = \frac{|2^{W-1}V_{W,B}(k)|}{|2^{W-1}V_{W,B}(1)|} = \frac{|V_{W,B}(k)|}{|V_{W,B}(1)|}$. That is, using dBc notation[2], the spur magnitude at k will be:

$$20\log_{10}|V_{W,B}(k)| - 20\log_{10}|V_{W,B}(1)| \text{ dBc.} \qquad (8)$$

Clearly, for $k \neq 0$, the value of (8) is negative. The spur magnitude is $20\log_{10}|V_{W,B}(1)| - 20\log_{10}|V_{W,B}(k)|$ dB down from the main components at $k = \pm 1$. Notice that the phase-truncation spur magnitudes in (8) depend *only* on the windowing function $V_{W,B}(k)$. For our particular $B = 2$ case, we simply evaluate (8) at the six points $k = \{(2^W \pm 1), (2\times 2^W \pm 1), (3\times 2^W \pm 1)\}$. To characterize the spurs for *any* frequency control word, we simply repeat this exercise for all possible values of B, $1 \le B \le (M - W)$. For an arbitrary B the sine or cosine DDS phase truncation spurs will be located at $k \in \{(d2^W \pm 1):\ \text{for } 1 \le d \le (2^B - 1)\}$.

Notice that, for quadrature DDS if we consider both outputs (sine and cosine) as a complex exponential sequence $cs'(n) = e^{j\frac{2\pi n}{2^W}} = \cos(\frac{2\pi n}{2^W}) + j\sin(\frac{2\pi n}{2^W})$ and if we characterize the DDS output spectrum via the complex-input DFT, then $|CS'_W(k)| = 2^W\delta(k-1)$ (rather than (7)) and the *absence* of the delta at $k = 2^W - 1$ in $|CS'_W(k)|$ reduces the set of spurs at the output of the DDS to the values of $k \in \{(d2^W + 1):\ \text{for } 1 \le d \le (2^B - 1)\}$. The sets of *spur magnitudes* for sine, cosine, and quadrature DDS are identical, as expected. In the case of sine or cosine DDS there are two corresponding spurs with identical magnitudes ($|S_{W,B}(k)|$ is symmetric around the origin) while in the case of quadrature DDS there is a single spur for a given magnitude.

The theory we have developed thus far allows one to identify the locations of all phase-truncation spurs and compute their magnitudes relative to the main component with the assistance of the windowing function $V_{W,B}$. The identification of the worst (i.e., the one having greatest magnitude) spur (or spurs) is usually the most critical issue when characterizing DDS spurs. Although the techniques developed in the preceding sections could be used to compute *all* of the spurs and we could then identify the worst one or ones by ordering them, this approach would require more time and effort than necessary. There is a much more powerful technique which directly identifies the locations of worst-case spurs and, through (8), enables one to directly calculate their magnitudes. Therefore, by using this method, the N worst phase-truncation spur magnitudes are calculated by evaluating (8) only N times. Hence, the magnitude of the worst spur, which also yields the SFDR, can be obtained by evaluating the windowing function *only once*.

Considering a sine or cosine DDS, we begin by referring to expression (8) and noticing that the worst spur is the one from the set $\{(d2^W \pm 1):\ \text{for } 1 \le d \le (2^B - 1)\}$ that maximizes the magnitude of windowing function $|V_{W,B}(k)|$. Using (6):

$$|V_{W,B}(k)| = \left|\frac{1 - e^{-j\frac{2\pi}{2^W}k}}{1 - e^{-j\frac{2\pi}{2^{(W+B)}}k}}\right| = \frac{\left|1 - e^{-j\frac{2\pi}{2^W}k}\right|}{\left|1 - e^{-j\frac{2\pi}{2^{(W+B)}}k}\right|}.$$

The result is a ratio of absolute values, each having the form $|1 - e^{j\theta}|$. If we view $|1 - e^{j\theta}|$ as the magnitude of the difference between two unit-length vectors, then it can be shown ([2] page 54) that $|1 - e^{j\theta}| = 2\sin\frac{\theta}{2}$, and we obtain the following convenient form for $|V_{W,B}(k)|$:

$$|V_{W,B}(k)| = \frac{\left|1 - e^{-j\frac{2\pi}{2^W}k}\right|}{\left|1 - e^{-j\frac{2\pi}{2^{(W+B)}}k}\right|} = \frac{\left|2\sin(\frac{\pi}{2^W}k)\right|}{\left|2\sin(\frac{\pi}{2^{(W+B)}}k)\right|} = \frac{\left|\sin(\frac{\pi}{2^W}k)\right|}{\left|\sin(\frac{\pi}{2^{(W+B)}}k)\right|}. \qquad (9)$$

[2] Definition of dBc is: dB relative to the carrier.

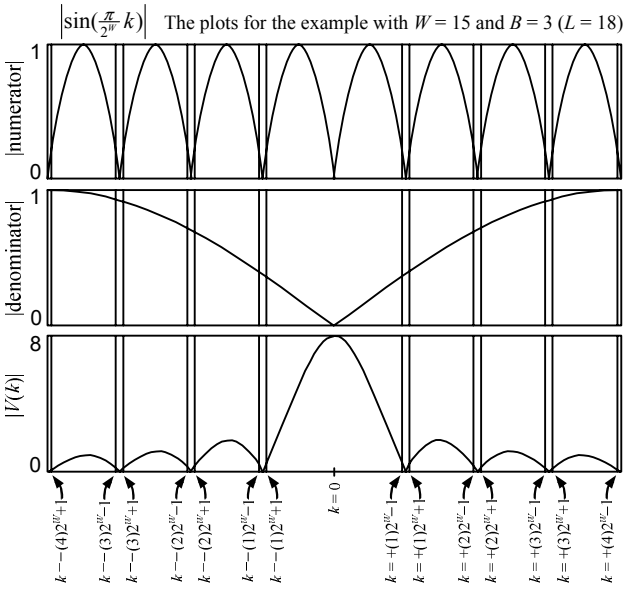

Figure 4. Phase-truncation spurs and the windowing function

We make the following observation about the denominator $\left|\sin(\frac{\pi}{2^{(W+B)}}k)\right|$ of (9). Since $\left|\sin\theta\right|$ is strictly monotone increasing for $0 \le \theta \le \frac{\pi}{2}$ and since $\frac{\pi}{2^{(W+B)}}k = \frac{\pi}{2}$ for $k = \frac{2^{(W+B)}}{2}$ we conclude that the denominator of (9) is strictly monotone increasing when k lies within the closed interval $[0, \frac{2^{(W+B)}}{2}]$. Similarly, since $\left|\sin\theta\right|$ is strictly monotone decreasing for $-\frac{\pi}{2} \le \theta \le 0$ and since $\frac{\pi}{2^{(W+B)}}k = -\frac{\pi}{2}$ for $k = -\frac{2^{(W+B)}}{2}$ we conclude that the denominator of (9) is strictly monotone decreasing when k lies within the closed interval $[-\frac{2^{(W+B)}}{2}, 0]$. Therefore, the denominator $\left|\sin(\frac{\pi}{2^{(W+B)}}k)\right|$ of (9) *increases* as the index k moves *away* from the origin. Next, we perform a similar analysis on the numerator of (9). Since $\left|\sin\theta\right|$ is zero for $\theta = d\pi$, where d is an arbitrary integer, $\left|\sin(\frac{\pi}{2^W}k)\right|$ is zero for $k = d2^W$. These zeros in the numerator create the nulls of our windowing function. Also, $\left|\sin(\frac{\pi}{2^W}k)\right|$ is symmetric (even symmetry) around these nulls. For phase-truncation spurs, what we actually care about are the points immediately to the right and immediately to the left of these nulls since these are the locations of the phase-truncation spurs, as indicated by the set $\{(d2^W \pm 1):\ \text{for } 1 \le d \le (2^B - 1)\}$. The following is a simple proof, showing that the value of the numerator in (9) is the same for all k where phase-truncation spurs occur. For $k \in \{(d2^W \pm 1):\ \text{for } 1 \le d \le (2^B - 1)\}$,

$$\left|\sin(\tfrac{\pi}{2^W}(d2^W + 1))\right| = \left|\sin(d\pi + \tfrac{\pi}{2^W})\right| = \left|\sin\tfrac{\pi}{2^W}\right|$$

and similarly, $\left|\sin(\frac{\pi}{2^W}(d2^W - 1))\right| = \left|\sin(d\pi - \frac{\pi}{2^W})\right| = \left|\sin\frac{\pi}{2^W}\right|$.

Therefore, the numerator of (9) is *constant* at the location of all phase truncation spurs and the denominator is strictly monotone increasing as k moves away from the origin. Hence, the *worst* (largest magnitude) phase-truncation spur is the one *closest* to the origin. For a sine or cosine DDS there are two largest-magnitude phase-truncation spurs located at $k = \pm(2^W - 1)$ and for a quadrature DDS the largest-magnitude phase-truncation spur is located at $k = -(2^W - 1)$. Furthermore, since the denominator is *strictly* monotone increasing as the index k moves away from the origin, it follows that *all* phase-truncation spurs, in each of the closed intervals $[-\frac{2^{(W+B)}}{2}, 0]$ and $[0, \frac{2^{(W+B)}}{2}]$, have *distinct* magnitudes, and that they arrange themselves from largest to smallest as their location moves away from the origin. This suggests that the N worst spurs could be calculated by evaluating the windowing function at the N phase truncation spur locations closest to the origin. Fig. 4 illustrates this point for a sine or cosine DDS with W = 15 and B = 3.

Since $\left|V(k)\right| = \left|V(-k)\right|$ (see (9)), the worst phase-truncation spur for sine, cosine, or quadrature DDS, relative to the main component, is therefore obtained by using (9) and evaluating (8) for $k = 2^W - 1$. The result is:

$$20\log_{10}\left|\sin(\tfrac{\pi}{2^{(W+B)}})\right| - 20\log_{10}\left|\sin(\pi(\tfrac{1}{2^B} - \tfrac{1}{2^{(W+B)}})\right| \text{ dBc.} \quad (10)$$

V. Spurs due to Arbitrary SCMF Non-Idealities in the Presence of Phase-Word Truncation

We can easily extend the analysis of Section IV to account for the spurs resulting from arbitrary SCMF non-idealities employed to facilitate efficient SCMF implementation. All arguments made in Section IV still hold when we have such a SCMF implementation, except that $S'_W(k)$ will have spurs *between* the previously discussed delta functions. The magnitudes of these spurs depend on the output precision and implementation details of the SCMF. Therefore, for frequency control words with $L > W$ (i.e., where there *is* phase-word truncation) the spurs in $S'_W(k)$ are also windowed by the windowing function $V_{W,B}(k)$. The expressions $s'(n)$, $\left|S'_W(k)\right|$, and $S_{W,B}(k)$ for an arbitrary non-ideal SCMF are:

$$\begin{aligned} s'(n) &= \sin(\tfrac{2\pi n}{2^W}) + q(n) \\ \left|S'_W(k)\right| &= a_0\delta(k) + a_1 2^{W-1}(\delta(k-1) + \delta(k-(2^W-1))) \\ &\quad + a_{2^{W-1}}\delta(k-2^{W-1}) + \sum_{i=2}^{2^{W-1}-1} a_i(\delta(k-i) + \delta(k-(2^W-i))) \\ S_{W,B}(k) &= V_{W,B}(k)S'_W(k) \end{aligned} \quad (11)$$

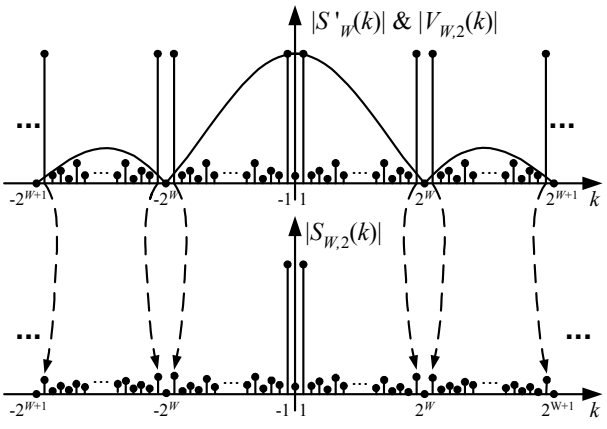

Figure 5. $V_{W,2}(k)$ over $S'_W(k)$ in a DDS with a non-ideal SCMF.

where $q(n)$ is the specific error sequence associated with the non-ideal SCMF, where a_1 is the distortion of the main components at $k = \pm 1$ (and $2^W \pm 1, \ldots$), where a_0 (DC spur) and a_2 through $a_{2^{W-1}}$ are the spur magnitudes in $S'_W(k)$. Since the sequence $s'(n)$ in (11) captures all SCMF non-idealities due to the specific implementation, we refer to it as the SCMF *signature sequence*. For sine or cosine DDS $s'(n)$ is a real-valued sequence, $|S'_W(k)| = |S'_W(-k)|$ (it is an even function). Therefore, the two main components $|S'_W(\pm 1)|$ in (11) have *identical* distortion a_1 and, in general, $|S'_W(\pm 1)| = |S'_W(d2^W \pm 1)|$ for any integer d. Consequently, the spur magnitude at $k = d2^W \pm 1$ relative to that of the desired sinusoid is: $\frac{|S_{W,B}(k)|}{|S_{W,B}(1)|} = \frac{|V_{W,B}(k)||S'_W(k)|}{|V_{W,B}(1)||S'_W(1)|} = \frac{|V_{W,B}(k)|}{|V_{W,B}(1)|}$. Hence the magnitudes of the spurs generated from phase-word truncation, relative to the main carrier magnitude, remain dictated by (8) (i.e., they are only a function of $V_{W,B}(k)$). That is, the phase truncation spur magnitudes (and locations) are *identical* for the ideal and non-ideal SCMF. Effectively, the set of spurs caused by phase truncation and the set generated from a non-ideal SCMF, relative to that of the main carrier components, are *disjoint*. The *only* spur not attenuated by $V_{W,B}(k)$ is the DC spur, hence (8) indicates the *increase* of the nonzero DC spur relative to the main components. In Section 5.4 of [2], it is shown that, when the SCMF is implemented to exploit the sine/cosine wave symmetry, the DC spur and all the spurs in even DFT frequency bin locations will be zero. Fig. 5 illustrates the general situation.

The theory developed thus far can be used to completely characterize *all* spurs due to phase truncation and non-ideal SCMF for any fcw with $L > W$ through the expressions (6). For fcw with large values of L (such as $L = 32$ or $L = 48$) the spectrum $S_{W,B}(k)$ will contain 2^L components. The characterization and storage of all 2^L components may require a prohibitively large amount of memory and computation. The computation necessary to characterize a single spur is small (6), but there are too many spurs. If *all* the spurs need to be characterized then one has no choice but to evaluate (6) for all $k = 0,1,\ldots,2^L - 1$. If, instead, the worst N spurs (for example the worst 100 spurs), or all spurs above a threshold (such as -100 dBc) need to be characterized, then the strictly monotone property of the windowing function, from Section IV, can be exploited to create a very fast algorithm.

Recall (11), which constructs the entire spectrum $S_{W,B}(k)$ by concatenating 2^B copies of $S'_W(k)$ and windowing them with $V_{W,B}(k)$. The main components of $S'_W(k)$ give rise to all phase-truncation spurs in $S_{W,B}(k)$, and every spur in $S'_W(k)$ gives rise to 2^B spurs in $S_{W,B}(k)$ (which are uniformly distributed in frequency at intervals of length 2^W). For the interval $[-2^{L-1}, 2^{L-1}]$ (equivalent to the interval $[0, 2^L]$ for the DFT,) from Section IV we know the denominator of $|V_{W,B}(k)|$ in (9) is strictly monotone increasing as k moves away from the origin. From Section IV we also know that the numerator of $|V_{W,B}(k)|$ is periodic in k with period 2^W. Therefore, since the set of 2^B spurs in $S_{W,B}(k)$ generated from *one* spur in $S'_W(k)$ are equally spaced at length-2^W intervals, we conclude that the numerator of $|V_{W,B}(k)|$ is constant at the positions of these spurs (see Fig. 4 for reference). Hence, similar to the phase-truncation spurs, the set of spurs created from *one* spur in $S'_W(k)$ arrange themselves with decreasing magnitudes as k moves away from the origin. This property can be used to create a fast algorithm for the characterization of the N worst spurs or all spurs above a specified threshold value. For a sine or cosine DDS, the following is the outline for a two-phase algorithm to accept an arbitrary SCMF signature sequence $s'(n)$, W, L, and N or spur magnitude threshold ε, and to generate the magnitudes and locations of the largest-magnitude spurs.

Phase I

1. Compute $|S'_W(k)|$ for $0 \le k < 2^W$.
2. Compute $|S_{W,B}(k)| = |V_{W,B}(k)||S'_W(k)|$ for $0 \le k < 2^W$ and sort in a vector *S_ord* in the order of decreasing magnitudes and keep track of the indices in a vector *k_ord*.
3. The first element of *k_ord* is 1, corresponding to the index of the main component, and the first element of *S_ord* will contain the magnitude of the main component. Save the magnitude of the main component and remove it from both *k_ord* and *S_ord*.

4. Construct a vector *potential_index_set* (which keeps track of the potential locations for the *next* worst spur) containing only the first element of *k_ord*. Remove that first element from *k_ord*. If $B>1$, then append *potential_index_set* with 2^W+1.
5. Create two vectors *spurs* and *locations* to store the magnitudes and locations of the worst spurs to be computed in Phase II.

Phase II

(Repeat these steps *N* times for the *N* largest-magnitude spurs, or repeat until the obtained spur is below the threshold ε to obtain all spurs above the threshold ε.)

1. Compute the spur magnitudes for the indices in *potential_index_set* using (6) and store the magnitude and location of the worst one in the vectors *spurs* and *locations* respectively.
2. **If** (the index of the worst spur from step 1 is less than 2^W), then, if $B>1$, increment that index in *potential_index_set* by 2^W. If $B=1$, then remove that index from *potential_index_set*. If the vector *k_ord* is not empty, remove its first element and add it to *potential_index_set* as well.

   Else If (the index of the worst spur from step 1 is greater than $2^{L-1}-2^W$), then remove it from *potential_index_set*.

   Otherwise, increment the index of the worst spur from step 1 in *potential_index_set* by 2^W.

□

Each spur magnitude in the vector *spurs* will appear twice on the DDS output spectrum since we considered a sine or cosine DDS. The corresponding element in vector *locations* will have the positive-index location and the second is simply the negative of that index. These spur locations, of course, correspond to a single-nonzero-bit fcw. To obtain the spur locations for any fcw with the given *L*, one may apply the rearrangement of (1) to the indices in vector *locations*. A similar outline for a quadrature DDS is found in Section 3.5.2 of [2].

VI. DDS SNR due to Arbitrary SCMF Non-Idealities in the Presence of Phase-Word Truncation

It is shown in Section 4.1 of [2] that two DDS with identical SFDR can have very different SNR since SFDR measures only the largest-magnitude spur while SNR collectively measures all the spurs. Therefore, the consideration of DDS output SNR in conjunction with SFDR is important.

The total power for any periodic time-domain sequence $x(n)$ can be computed directly as $P=\frac{1}{N}\sum_{n=0}^{N-1}\left|x(n)\right|^2$, or from its DFT $X(k)$ as $P=\frac{1}{N^2}\sum_{k=0}^{N-1}\left|X(k)\right|^2$, where *N* is the period of $x(n)$. For fcw with common rightmost-nonzero-bit position *L*, since the DDS outputs and their spectra are just the rearrangements of each other dictated by (1), we conclude that they have identical total power. Furthermore, since their signal power is dictated solely by the squared magnitude of their corresponding main DFT components, and the main DFT components are also rearrangements of one another, we conclude that their signal powers are also identical. Hence, their total noise powers $P_{Noise}=P_{Total}-P_{Signal}$ must also be identical. Therefore, the SNR=$\frac{P_{Signal}}{P_{Noise}}$ for all fcw with a common rightmost-nonzero-bit position can be computed by considering the single-nonzero-bit fcw.

Considering a sine or cosine DDS, for the single-nonzero-bit fcw, the signal power $P_{SIGNAL}=\frac{1}{2^{(2W+2B)}}\left|S(1)\right|^2+\frac{1}{2^{(2W+2B)}}\left|S(2^{(W+B)}-1)\right|^2$ resides in the deltas corresponding to the main frequency components and the magnitudes of these deltas are identical as shown in Section V (i.e., $\left|S(1)\right|=\left|S(2^{(W+B)}-1)\right|$). Therefore, by using (6) we can express the signal power as

$$P_{SIGNAL}=\frac{2}{2^{(2W+2B)}}\left|V(1)S'(1)\right|^2. \qquad (12)$$

Using the fact that $s(2^Bn)=s(2^Bn+1)=\ldots=s(2^Bn+2^B-1)=s'(n)$, as discussed in Section III, the total power $P_{TOTAL}=\frac{1}{2^{(W+B)}}\sum_{n=0}^{2^{(W+B)}-1}\left|s(n)\right|^2$ can be rewritten in terms of the signature sequence $s'(n)$. The result is $P_{TOTAL}=\frac{1}{2^W}\sum_{n=0}^{2^W-1}\left|s'(n)\right|^2$ and, using Parseval's theorem, it can also be written in terms of $S'(k)$ as $\frac{1}{2^{2W}}\sum_{k=0}^{2^W-1}\left|S'(k)\right|^2$. Subtracting the signal power (12) from the total power, we obtain the *total* noise power (that due to both SCMF non-idealities and phase truncation):

$$P_{NOISE}=\frac{1}{2^W}\sum_{n=0}^{2^W-1}\left|s'(n)\right|^2-\frac{2}{2^{(2W+2B)}}\left|V(1)S'(1)\right|^2$$

or

$$P_{NOISE}=\frac{1}{2^{2W}}\sum_{k=0}^{2^W-1}\left|S'(k)\right|^2-\frac{2}{2^{(2W+2B)}}\left|V(1)S'(1)\right|^2.$$

Hence, the SNR $=\frac{P_{SIGNAL}}{P_{NOISE}}$ in dB can be expressed as:

$$\mathrm{SNR}=10\log_{10}\frac{\left|V(1)S'(1)\right|^2}{2^{(W+2B-1)}\sum_{n=0}^{2^W-1}\left|s'(n)\right|^2-\left|V(1)S'(1)\right|^2} \qquad (13\text{ a})$$

or

$$\mathrm{SNR}=10\log_{10}\frac{\left|V(1)S'(1)\right|^2}{2^{(2B-1)}\sum_{k=0}^{2^W-1}\left|S'(k)\right|^2-\left|V(1)S'(1)\right|^2}. \qquad (13\text{ b})$$

Since the windowing function V and the signature sequence $s'(n)$ for an arbitrary SCMF enter into the expressions (13), the impact of both phase truncation and arbitrary SCMF non-idealities on the DDS output SNR are considered in (13). Different DDS implementations with identical phase truncation and identical output precision can have substantially different SNR since different implementations of the SCMF can give rise to different signature sequences $s'(n)$. Notice that (13) computes the SNR exactly (i.e., without use of any approximations,) and it corresponds specifically to the SCMF implementation giving rise to the signature sequence $s'(n)$ used in (13).

For quadrature DDS, the only difference in the derivation of their SNR expression is that it has a single main component instead of two main components as in the case of a sine or cosine DDS. The SNR expressions corresponding to quadrature DDS are similarly derived in Section 4.2 of [2] to be

$$\mathrm{SNR} = 10\log_{10}\frac{|V(1)\,CS'(1)|^2}{2^{(W+2B)}\sum_{n=0}^{2^W-1}|cs'(n)|^2 - |V(1)\,CS'(1)|^2} \qquad (14\text{ a})$$

or

$$\mathrm{SNR} = 10\log_{10}\frac{|V(1)\,CS'(1)|^2}{2^{(2B)}\sum_{k=0}^{2^W-1}|CS'(k)|^2 - |V(1)\,S'(1)|^2}. \qquad (14\text{ b})$$

Therefore, evaluating (13) or (14) for the given W and the given signature sequence and all possible values of B, where $1 \le B \le (M-W)$, yields the SNR for *all* fcw resulting in phase-word truncation. Computation of SNR for fcw resulting in no phase-word truncation (i.e., fcw with $L \le W$) is easier due to their considerably shorter period of the DDS output. A thorough treatment of SNR computation for such fcw and relevant initial phase conditions can be found in Section 4.6 of [2].

A Major Practical Issue: A point of major importance is that the SNR expressions (13) and (14) are computationally very efficient. In practice, the sequence at the output of a DDS has a (large!) period of $2^{(W+B)}$ samples, therefore its direct SNR computation using summations for the power of the DDS output sequence is proportional to $2^{(W+B)}$. Since the expressions (13) and (14) are computed from the windowing function V and the related signature sequence with a period of 2^W samples, the computational complexity of (13) and (14) is proportional to 2^W. Therefore, the SNR expressions (13) and (14) are more efficient by a factor of 2^B. This efficiency factor is crucial since B, for practical DDS implementations, is typically as large as 18 or more. This large efficiency factor makes the exact evaluation of the SNR, e.g. by expressions (13) and (14), feasible.

It is also shown in Section 4.3 of [2] that (13) and (14) are decreasing functions of B. Therefore, evaluating (13) and (14) for $B=1$ and $B=M-W$ will yield the maximum and minimum SNR bounds, respectively, for fcw with $L > W$. Other useful SNR bounds are derived in Sections 4.3 - 4.5 of [2].

VII. Conclusions

A simple and fast (patent pending) algorithm is presented for the exact computation of DDS output spur magnitudes and locations, SFDR, and SNR, in the presence of both phase-word truncation and arbitrary implementation of the DDS since/cosine mapping function (SCMF). A key windowing function provides the means to compute an arbitrary number of largest-magnitude spurs and the total power of the DDS output spectrum *without generating the entire spectrum*. Sections 3.7 and 4.7 of [2] use the presented algorithm and SNR expressions (13) and (14) for phase-truncation causing fcw, along with even simpler algorithms for non-phase-truncation causing fcw to perform a complete DDS analysis for an arbitrary DDS (i.e., arbitrary SCMF implementation) having the general form of Fig. 1. This complete DDS analysis on an ordinary personal computer takes approximately one minute.

References

[1] A. Torosyan and A. N. Willson, Jr., "Analysis of the output spectrum for direct digital frequency synthesizers in the presence of phase truncation and finite arithmetic precision," in *Proc. 2-nd Image and Signal Processing and Analysis Conference*, 2001, pp. 458-463.

[2] A. Torosyan, *Direct Digital Frequency Synthesizers: Complete Analysis and Design Guidelines*, Ph.D. Dissertation, University of California, Los Angeles, 2003.

[3] J. Tierney, C. M. Rader, and B. Gold, "A digital frequency synthesizer," *IEEE Transactions on Audio and Electroacoustics*, vol. AU-19, pp. 48-57, March 1971.

[4] H. T. Nicholas and H. Samueli, "A 150-MHz direct digital frequency synthesizer in 1.25-µm CMOS with –90 dB spurious performance," *IEEE J. Solid State Circuits*, vol. 26, pp. 1959-1969, December 1991.

[5] A. Madisetti, A. Kwentus, and A. N. Willson, Jr., "A 100-MHz 16-b, direct digital frequency synthesizer with a 100-dBc spurious-free dynamic range," *IEEE Journal of Solid-State Circuits*, vol. 34, pp. 1034-1043, August 1999.

[6] S. Mehrgardt, "Noise spectra of digital sine-generators using the table-lookup method," *IEEE Trans. Acoustics, Speech, and Signal Processing*, vol. 31, pp. 1037-1039, August 1983.

[7] H. T. Nicholas, *The Determination of the Output Spectrum of Direct Digital Frequency Synthesizers in the Presence of Phase Accumulator Truncation*, M.S. thesis, University of California, Los Angeles, 1985.

[8] H. T. Nicholas and H. Samueli, "An analysis of the output spectrum of direct digital frequency synthesizers in the presence phase-accumulator truncation," in *Proc. 41-st Annual Frequency Control Symposium*, 1987, pp. 495-502.

[9] Y. C. Jenq, "Digital spectra of nonuniformly sampled signals – digital look-up tunable sinusoidal oscillators," *IEEE Trans. Instrumentation and Measurement*, vol. 37, pp. 358-362, September 1988.

[10] V. F. Kroupa, "Discrete spurious signals and background noise in direct digital frequency synthesizers," in *IEEE Proc. International Frequency Control Symposium*, 1993, pp. 242-250.

[11] S. C. Kak and N. S. Jayant, "On speech encryption using waveform scrambling," *Bell System Technical Journal*, vol. 56, pp. 781-808, May-June 1977.